Modeling, Identification and Validation of the Modified Magnetic Levitation Model

Tomáš TKÁČIK[1], *Anna JADLOVSKÁ*[1], *Ján JADLOVSKÝ*[1]

[1]Department of Cybernetics and Artificial Intelligence, Faculty of Electrical Engineering and Informatics, Technical University in Košice, Letná 9, 042 00 Košice, Slovak Republic

tomas.tkacik@tuke.sk, anna.jadlovska@tuke.sk, jan.jadlovsky@tuke.sk

DOI: 10.15598/aeee.v22i1.5261

Article history: Received Jun 03, 2023; Revised Oct 09, 2023; Accepted Jan 29, 2024; Published Mar 31, 2024.

Abstract. *This paper presents the nonlinear system identification methodology on the Modified magnetic levitation model (MLM). The proposed modification of the original CE 152 MLM replaces the outdated MF624 laboratory card with the Board51. This modification enables the integration of the MLM into the Distributed Control Systems (DCS) architecture and moves the control loop closer to the system. The integration into the DCS architecture requires a detailed description of the system, which along with well-known physics laws is used by the analytical identification method to derive a mathematical model. The method of experimental identification is used to estimate all four unknown parameter values of the derived mathematical model. Parameters are estimated in the structure of output prediction error using the nonlinear least squares method. The resulting gray-box model is used to design a stabilizing optimal state control algorithm (LQI). This control algorithm is used for indirect validation of the identified model by comparing the outputs of the real and simulation models in a closed-loop setup. The validated model can be used as the basis for the creation of the digital twin.*

Keywords

Distributed control systems, experimental identification, magnetic levitation model, optimal state control, parameter estimation.

1. Introduction

The magnetic levitation systems use magnetic force to levitate an object without any physical link to it. In general, a careful balance of all forces acting on the object is required to keep the object still. Since forces acting on the object may change due to external disturbances, an active compensation is required [1]. In the case of magnetic levitation systems, an electromagnet is used to produce a magnetic force of varying strength adjusted based on the position of the object. Applications of magnetic levitation systems include contact-less position control, for example, magnetic bearings, magnetic levitation trains, particle accelerators [2], precision control rod position control in nuclear reactors [3], artificial heart pumps [4], etc.

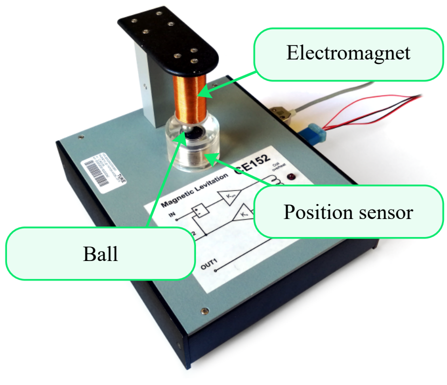

Fig. 1: Overview of the CE 152 Magnetic levitation model by the Humusoft company [5].

Magnetic levitation systems are of a big interest in the control engineering discipline. The reasons are a simple construction and a straightforward working principle. On the other hand, these systems are challenging in identification and control tasks [6], mainly due to the fast system dynamics and open-loop instability. Such systems are part of many research groups across the world. In our research group, the Center of Modern Control Techniques and Industrial Informatics (CMCT&II) at the Department of Cybernetics and Artificial Intelligence (DCAI) at the Technical University of Košice (TUKE), the CE 152 Magnetic levitation model [5] created by the Humusoft company has already been used in research and education activities. This includes the derivation of the mathematical model using physics laws, parameter identification using genetic algorithms, and control design using feedback linearization method [7]. The CE 152 system by Humusoft consists of a Magnetic levitation model (see Fig. 1), a Power supply, and the MF624 PCI multifunction IO card. Similar models available are made by other well-known companies, such as Quanser [8], Feedback Instruments [9], or Bytronic [10]. These models are primarily used for educational purposes with software toolboxes supporting modeling, identification, and control tasks [11].

The focus of this paper is to present nonlinear system identification methodology on the Modified CE 152 Magnetic levitation model (MLM, see Fig. 2) and its integration into the DCS architecture at the CMCT&II DCAI [12]. The main motivation for the modification was the outdated MF624 IO card that needed a replacement. A replacement in the form of the Board51 is proposed, which enables better integration of the system into the DCS architecture. Integration into DCS architecture requires detailed analysis of all components deepening the understanding of the MLM that can be helpful for system modeling.

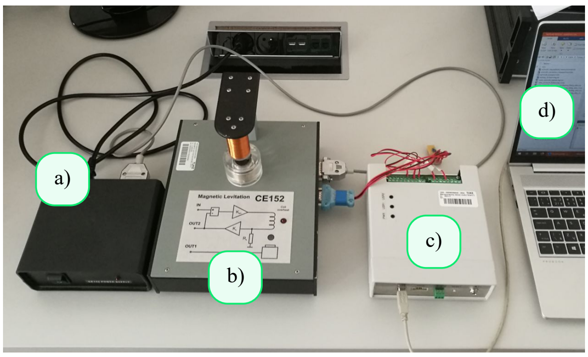

Fig. 2: The Modified CE 152 MLM; a) Power supply; b) Magnetic levitation model; c) Board51 with enclosure; d) PC.

The presented methodology of nonlinear system identification, which includes system modeling, parameter identification, and identified model validation is used to verify the Modified MLM. The standard approach in system modeling is the first principle modeling that uses physics laws to derive mathematical model, see [1], [13], and [14]. In all cases, the resulting mathematical model incorporated a few simplifications to make the model more manageable. On the contrary, authors in [15] used extensive physics analysis to derive a mathematical model that includes interactions between the electromagnet and metallic ball. Although such a model has better approximation capabilities, which are favorable in state estimation and predictive control tasks [16], it is more challenging to estimate its parameter values. Model parameters can be estimated using simple experiments by taking measurements at special points, where differential equations can be transformed into algebraic, like in [6], [13] and [17]. Previously, genetic algorithms have been used to estimate parameter values using data capturing the system dynamics [7]. An alternative approach was taken by authors of [6] and [18], where they used purely data-driven methods to create a black-box model with good results. However, operating the system without sufficient knowledge may pose risk to operators or the system itself. To balance model accuracy and complexity, it was decided to use first principles modeling with simplified physical laws.

In this paper, the least squares method is used to estimate parameter values of the mathematical model from experimental data capturing the system dynamics. Measured data from the MLM has been split into multiple shorter experiments that mainly excluded situations when the ball position is saturated. This improved the performance of the selected parameter estimation method. Selected option employs both physical insight and data-driven methods. The identified gray-box model needs to be validated, which is usually done in a control structure. Many control algorithms have been applied to MLMs, e.g. PID in [1], [6] and [14], state space control in [18], optimal control in [1] and [18], model predictive control in [14], [16] and [18], fuzzy control [18], artificial neural network control in [1], [6] and [19], etc. To validate the gray-box model, an LQI control algorithm is chosen as in the validation of the Aerodynamic levitation system [21]. The optimal control algorithm is easy to design and implement, while being sufficiently robust for MLM [7]. The identified gray-box model is the basis for the creation of a digital twin of the MLM.

The CE 152 MLM, Aerodynamic levitation model, and CE 150 Helicopter model [20] are part of the Research & Development (R&D) platform at CMCT&II DCAI. This platform is used for the evaluation of system identification methods and control algorithms using classical and intelligent approaches.

This paper is organized as follows. Section 2 presents the MLM from hardware side. This includes description of proposed hardware modification and integration into the DCS architecture at the CMCT&II. Section 3 presents a methodology of the system identification applied to the Modified MLM. The methodology includes mathematical modeling, parameter estimation, and gray-box model validation steps. Finally, Section 4 summarizes key points of the presented research and outlines future research options in the design of advanced identification and control algorithms.

2. Description of Modified Magnetic Levitation Model

From a physical perspective, the CE 152 Magnetic levitation model consists of the following components: Magnetic levitation model (Fig. 1), Power supply, and MF624 IO card. The magnetic levitation model can be subdivided into two subsystems - the *power amplifier subsystem* and the *ball & coil subsystem*, that will be described in detail later. The Power supply provides the MLM with an adequate amount of power since huge power spikes are required to energize the electromagnet rapidly. The MF624 IO card is a PCI expansion card that extends the computer's interfaces with both digital and analog I/O. These additional capabilities can be used with a dedicated software library or directly with the MATLAB/Simulink software. A clear disadvantage of this solution is the need for a computer with an obsolete PCI interface. Also, a control loop is running on a standard Windows operating system, which is not a real-time operating system. This means that the sampling period T_s may change based on the overall system load. The authors in [18] replaced the MF624 with the Arduino Due development board. With suitable MATLAB toolboxes, this configuration allows using Simulink blocks directly without writing a single line of code for the Arduino. Although generated code can be exported and manually modified, such implementation comes with a performance penalty. Similarly to the original solution, the Arduino Due behaves as a simple IO interface for the computer.

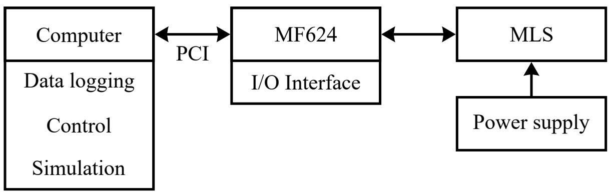

(a)

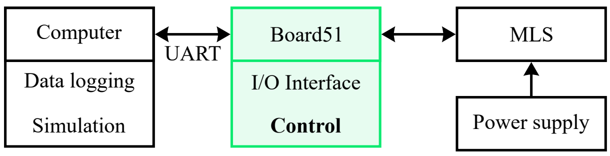

(b)

Fig. 3: Comparison of (a) Original structure of the Magnetic levitation model and (b) Modified structure of the Magnetic levitation model.

The proposed solution replaces the MF624 IO card with the Board51 general purpose data acquisition board [22]. This board is built around the 8051 microcontroller that have all required I/O interfaces to control the MLM. Due to the limited amount of program memory of the microcontroller, all control and estimation algorithms must be implemented in the C language. Running such algorithms on the microcontroller guarantees a fixed sampling period T_s and also makes the MLM portable. Moreover, system states can be logged and control commands can be sent over the UART interface. Comparison of original and proposed system structure is shown in Fig. 3.

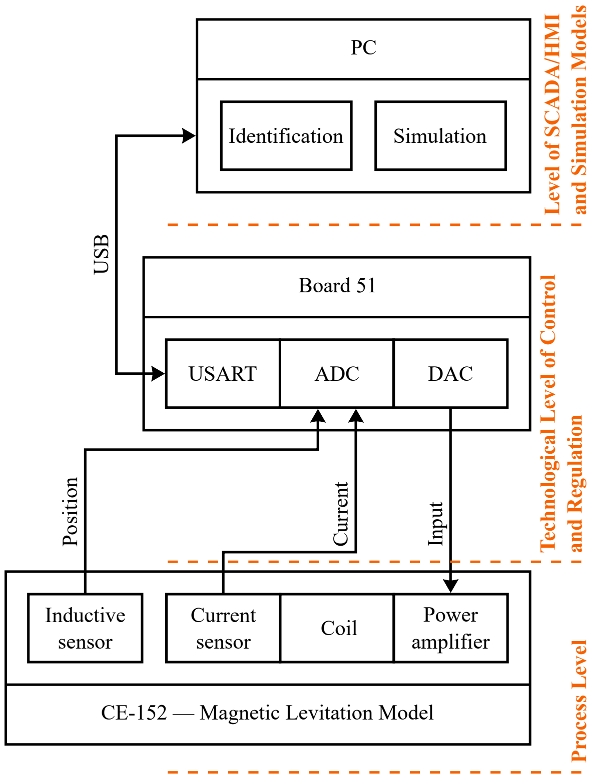

Fig. 4: The Modified magnetic levitation model implemented into the DCS architecture.

2.1. Implementation of the Modified MLM into the DCS Architecture

The DCS architecture at the CMCT&II DCAI represents an example of the Cyber-physical system for intelligent manufacturing [23], which is built over the collection of laboratory models (e.g. Modified MLM, Aerodynamic levitation model, Helicopter model, Mobile robots, Ball and plate model, etc.). DCS presents a hierarchical architecture consisting of five technological levels described in detail in [12].

To implement the Modified MLM (Fig. 3) into the DCS architecture, the first three levels of DCS are customized. On the *Process Level* are situated the inductive sensor, current sensor, coil, and power amplifier. On the *Technological Level of Control and Regulation*, the control algorithms are implemented into the Board51. *The Level of SCADA/HMI and Simulation Models* contains functions for parameter estimation, control algorithm synthesis, and simulation validation of the gray-box model. Figure 4 shows the implementation of the Modified MLM into DCS architecture. Such implementation into the DCS architecture creates a communication interface that is required to create a digital twin of the MLM [24].

3. Identification Methodology of the Modified MLM

The proposed Modified MLM must be identified and validated before it can be used in research and education activities, such as the design of control algorithms. The identification methodology consists of the following steps: derivation of the mathematical model of the nonlinear system, parameter identification using methods of experimental identification, and model validation in the closed-loop structure.

3.1. Mathematical modeling

The MLM consists of the *power amplifier subsystem* and the *ball & coil subsystem*. Both subsystems are connected sequentially with minimal interactions, which makes it possible to model them individually.

The *power amplifier subsystem* is an electrical system, whose goal is to control coil current $i_c(t)$ [A] based on the input voltage $u_c(t)$ [V]. The electromagnet's coil can be approximated using ideal inductor with an ideal resistor connected in series. Authors in [1], [15] and [19] pointed out that the coil's inductance changes in presence of the steel ball. Also during the operation, the coil's temperature rises and thus its resistance rises too. These changes are generally too small to have a significant influence on system dynamics, therefore are considered constant. The coil is connected to the circuit consisting of a shunt resistor and a series of operational amplifiers, see Fig. 5. This configuration allows the coil current $i_c(t)$ to be directly measured to adjust the power to the coil in a feedback loop. A mathematical model of the *power amplifier subsystem* is presented in [5] and [13]. Its disadvantage is a plethora of unknown parameters that must be experimentally estimated. Therefore, a suitable approximation in form of 1st order linear differential equation was chosen:

$$T_A \frac{di_c(t)}{dt} + i_c(t) = K_A u_c(t), \tag{1}$$

where K_A $[\mathrm{A} \cdot \mathrm{V}^{-1}]$ is a gain of the *power amplifier* and T_A [s] is its time constant. The authors in [7], [14] and [17] decided to ignore the dynamics of the *power amplifier subsystem* altogether due to fast dynamics compared to the utilized sampling period $T_s = 0.002$ [s].

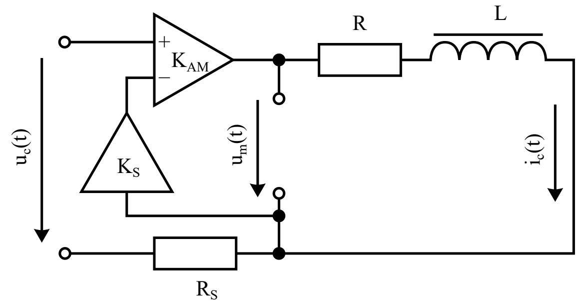

Fig. 5: Scheme of the power amplifier subsystem.

The *ball & coil subsystem* is a mechanical system whose structure is shown in Fig. 6. Its main component is a steel ball that can move freely between the electromagnet on the top and the position sensor on the bottom. By finding all forces acting on the ball, the subsystem's model can be derived using Newton's second law $F(t) = ma(t)$, where $F(t)$ [N] is force acting on the object, m [kg] is object's weight, and $a(t) = \ddot{x}(t)$ $[\mathrm{m} \cdot \mathrm{s}^{-2}]$ is object's acceleration. The following three forces are considered: gravitational force F_g [N], magnetic force $F_m(t)$ [N], and drag force $F_d(t)$ [N]. Combining all forces with correct signs into single equation results in a force balance equation:

$$F(t) = F_m(t) - F_d(t) - F_g, \tag{2}$$

of the *ball & coil subsystem*. Signs are based on selected convention, where the bottom-most position is equal to zero and the top-most position is x_{max} [m].

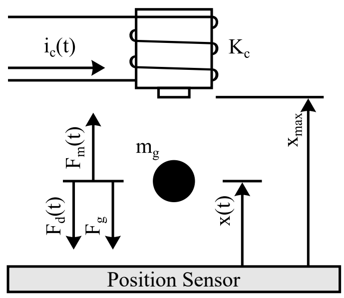

Fig. 6: Structure of the ball & coil subsystem.

The magnetic force $F_m(t)$ is directly proportional to the coil constant K_c $[\mathrm{N} \cdot \mathrm{m}^2 \cdot \mathrm{A}^{-2}]$ and the squared coil current $i_c^2(t)$, and inversely proportional to the squared distance between the ball and the coil $(x(t) - x_{max})^2$, where $x(t)$ [m] is the ball position. The coil constant K_c combines a number of fixed value parameters related to the electromagnet like the number of turns, the cross-section area, and the permeability of its core. The magnetic force $F_m(t)$ is described as follows:

$$F_m(t) = \frac{K_c i_c^2(t)}{(x(t) - x_{max})^2}. \tag{3}$$

The gravitational force F_g described by:

$$F_g = m_g g, \tag{4}$$

is constant as the ball's weight m_g [kg] and the gravitational acceleration g $[\mathrm{m \cdot s^{-2}}]$ are both constants. The drag force $F_d(t)$ combines aerodynamic drag force and drag force caused by the movement of a metallic object in the magnetic field. Although these forces are directly proportional to the square of the ball speed $v(t) = \dot{x}(t)$ $[\mathrm{m \cdot s^{-1}}]$, a linear effect is considered due to low speeds. To quantify this force, a combined drag coefficient b $[\mathrm{kg \cdot m^{-1}}]$ is introduced as follows:

$$F_d(t) = b\dot{x}(t). \tag{5}$$

By adding (3), (4), and (5) into (2) and rearranging components, the mathematical model of the *ball & coil subsystem* is derived:

$$m_g \ddot{x}(t) + b\dot{x}(t) = \frac{K_c i_c^2(t)}{(x(t) - x_{max})^2} - m_g g. \tag{6}$$

A complete mathematical model of the MLM is defined by differential equations (1) and (6) with system variables being coil current $i_c(t)$, ball position $x(t)$, ball speed $\dot{x}(t)$, ball acceleration $\ddot{x}(t)$, and input voltage $u_c(t)$ being a system input. Such a model is still missing parameter values, namely K_A, T_A, K_c, and b, that need to be estimated experimentally.

3.2. Estimation of Model Parameters

The next step in the identification methodology is parameter estimation. The goal of the experimental identification in general is to identify model structure and parameters purely from the measured data [25]. Since the model structure is defined by (1) and (6), only the parameters need to be estimated. The parameter estimation is a data-driven process. Its goal is to find parameter values so the behavior of the mathematical model closely matches the behavior of the real system [26]. The estimation process is formulated as an optimization task to minimize a cost function:

$$V(\boldsymbol{\varphi}) = \sum_{k=1}^{N} \left(\boldsymbol{y}(k) - \hat{\boldsymbol{y}}(k, \boldsymbol{\varphi})\right)^T \left(\boldsymbol{y}(k) - \hat{\boldsymbol{y}}(k, \boldsymbol{\varphi})\right), \tag{7}$$

where $\boldsymbol{y}(k)$ is a vector of measured values of the real system, $\hat{\boldsymbol{y}}(k)$ is the mathematical model output, and $\boldsymbol{\varphi}$ is a vector of parameters that need to be estimated. Although the real system and the mathematical model are continuous in time, the output variables can be sampled only at discrete time intervals. Therefore all signals are sampled using the same sampling period T_s. This method of parameter identification is referred to as gray-box identification driven by the output prediction error [25]. It is implemented in *greyest* and *nlgreyest* functions of the System Identification Toolbox in MATLAB. The difference between these functions is that the *nlgreyest* is more general as it can handle nonlinear models. Similar to the mathematical modeling, parameters of the *power amplifier subsystem* and the *ball & coil subsystem* can be estimated separately, as the outputs of both subsystems can be measured simultaneously. Such separation decreases the number of parameters that need to be estimated at once which significantly reduces computational complexity.

The *power amplifier subsystem* is linear and stable in the open-loop configuration. Therefore unknown parameters (K_A and T_A) from (1) can be estimated by analyzing step response. This can be done graphically or numerically [25]. The graphical approach was used to estimate amplifier gain K_A and numerical optimization to estimate the time constant T_A. The reason for this combination was the inability of the numerical method to estimate gain K_A correctly due to the unusual shape of the step response. Also, data needed to be sampled at a much higher rate (25 kHz) using an oscilloscope.

Parameter estimation of the *ball & coil subsystem* is more challenging. This is due to the fast and unstable dynamics of the subsystem and also a limited range of the ball position $x(t)$. The sawtooth signal was used to make an initial estimate of the coil constant K_c based on finding an equilibrium point - the point where magnetic $F_m(t)$ and gravitational F_g forces are equal:

$$m_g g = \frac{K_c i_c^2(t)}{(0 - x_{max})^2}. \tag{8}$$

The equilibrium point is experimentally determined from the data as the point right before the ball position $x(t)$ starts to change from its base position due to the magnetic force $F_m(t)$. Since the ball is stationary at that point the drag force $F_d(t)$ can be ignored.

Later, the drag coefficient b was estimated using the *nlgreyest* function of the System Identification Toolbox in MATLAB as the response to the pseudorandom binary signal. Since this function can not handle saturation of the ball position $x(t)$, it was necessary to split measured data into multiple experiments. This helped to avoid unwanted crossings of position limits. For the validation, models of both subsystems, the *power amplifier* (1) and *ball & coil* (6), with estimated parameters (K_A, T_A, b, and K_c) were implemented in the Simulink environment including saturation of the ball position $x(t)$ to make simulations more realistic.

3.3. Model validation in closed-loop setup

The final step of the system identification methodology is the model validation, which can be performed in open-loop and closed-loop configurations. The open-loop validation of the *power amplifier subsystem* and the *ball & coil subsystem* models as the response to the rectangular input voltage $u_c(t)$ signal is shown in Fig. 7 and Fig. 8 respectively. The oscillations of the ball position $x(t)$ in Fig. 8b are caused by the ball bouncing of the position sensor.

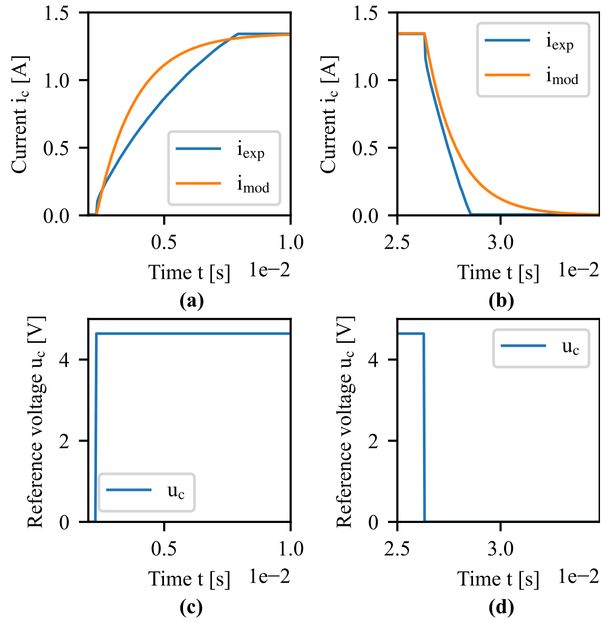

Fig. 7: Open-loop validation of the power amplifier subsystem; (a) and (b) system response; (c) and (d) system input.

Since results of the open-loop validation were inconclusive, the closed-loop validation in control structure was chosen. This requires designing a stabilizing control law first and then comparing the results. An LQI controller was chosen for this task, as it had been previously successfully applied in the verification of the Aerodynamic levitation model in [21]. In that particular case, the Kalman filter was utilized to estimate unmeasured state variables and to filter noise. Due to short sampling time T_s in case of the MLM and performance limitations of the Board51, a difference estimator is used to estimate ball speed $\dot{x}(t)$. The remaining state variables (coil current $i_c(t)$ and ball position $x(t)$) are measured directly.

To design an LQI control law, the following substitution of state variables was proposed:

$$x_1(t) = i_c(t);\ x_2(t) = x(t);\ x_3(t) = \dot{x}(t). \tag{9}$$

Then the state vector $\boldsymbol{x}(t)$ was defined as follows:

$$\boldsymbol{x}(t) = \begin{bmatrix} x_1(t) & x_2(t) & x_3(t) \end{bmatrix}^T. \tag{10}$$

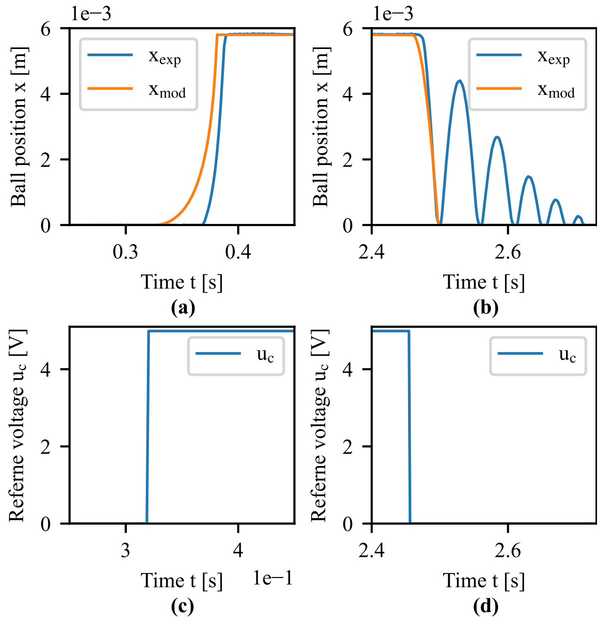

Fig. 8: Open-loop validation of the ball & coil subsystem; (a) and (b) system response; (c) and (d) system input.

The mathematical model (1) and (6) was transformed into a set of 1st order nonlinear differential equations:

$$\begin{aligned} \dot{x}_1(t) &= -\frac{1}{T_A}x_1(t) + \frac{K_A}{T_A}u_c(t) \\ \dot{x}_2(t) &= x_3(t) \\ \dot{x}_3(t) &= -\frac{b}{m_g}x_3(t) + \frac{K_c}{m_g}\frac{x_1^2(t)}{(x_2(t)-x_{max})^2} - g \end{aligned}, \tag{11}$$

which can be rewritten in a vector form:

$$\dot{\boldsymbol{x}}(t) = \boldsymbol{f}\left(\boldsymbol{x}(t), u_c(t)\right), \tag{12}$$

where $\boldsymbol{f}(\cdot)$ is a vector function defining the nonlinear dynamical system, which was linearized in the appropriate operation point $\boldsymbol{OP}$ by the first-order Taylor series expansion. The appropriate operation point:

$$\boldsymbol{OP} = \begin{bmatrix} x_{10} & x_{20} & x_{30} & u_{c0} \end{bmatrix}, \tag{13}$$

was chosen where the ball position $x_2(t)$ is exactly in the middle of its operating range and its speed $x_3(t)$ is zero. The coil current $x_1(t)$ and corresponding input voltage $u_c(t)$ were calculated from (11) with all derivatives on left hand side equal to zero ($\dot{\boldsymbol{x}}(t) = \boldsymbol{0}$). The resulting perturbation state space model:

$$\begin{aligned} \Delta\dot{\boldsymbol{x}}(t) &= \boldsymbol{A}\Delta\boldsymbol{x}(t) + \boldsymbol{B}\Delta u_c(t) \\ \Delta\boldsymbol{y}(t) &= \boldsymbol{C}\Delta\boldsymbol{x}(t) \end{aligned}, \tag{14}$$

is a linear approximation of (12) around the operation point $\boldsymbol{OP}$, where $\Delta\boldsymbol{x}(t) = (\boldsymbol{x}(t) - \boldsymbol{x_{OP}})$, $\Delta u_c(t) = (u_c(t) - u_{OP})$, and $\boldsymbol{C} = \boldsymbol{I}^{2\times3}$ is the output matrix. To use digital control directly built into the Board51, the model needs to be discretized first. This is done using

MATLAB's *c2d* function with the selected sampling period T_s to get:

$$\begin{aligned}\Delta\boldsymbol{x}(k+1) &= \boldsymbol{A_d}\Delta\boldsymbol{x}(k) + \boldsymbol{B_d}\Delta u_c(k)\\ \Delta\boldsymbol{y}(k) &= \boldsymbol{C}\Delta\boldsymbol{x}(k)\end{aligned}. \tag{15}$$

The discrete model (15) cannot be directly used to design the LQI control law, as the LQI control algorithm requires a model in the extended form. The following modification is proposed:

$$\Delta\boldsymbol{x_i}(k+1) = \boldsymbol{A_i}\Delta\boldsymbol{x_i}(k) + \boldsymbol{B_i}\Delta u_c(k), \tag{16}$$

where $\boldsymbol{A_i} = \begin{bmatrix}\boldsymbol{A_d} & 0\\ [0 \quad -T_s \quad 0] & 1\end{bmatrix}$, $\boldsymbol{B_i} = \begin{bmatrix}\boldsymbol{B_d}\\ 0\end{bmatrix}$, and $\Delta\boldsymbol{x_i}(k) = \left[\Delta\boldsymbol{x}^T(k) \quad (x_{ref}(k) - x_2(k))\right]^T$.

The LQI control algorithm belongs to group of optimal control algorithms, that are designed by minimizing quadratic criteria:

$$\begin{aligned}&V_{LQI}(\Delta\boldsymbol{x_i}, \Delta\boldsymbol{u_i}) =\\ &= \textstyle\sum_{k=0}^{\infty}\left(\Delta\boldsymbol{x_i}^T(k)\boldsymbol{Q}\Delta\boldsymbol{x_i}(k) + \Delta u_c^T(k)\boldsymbol{R}\Delta u_c(k)\right),\end{aligned} \tag{17}$$

where $\boldsymbol{Q}$ and $\boldsymbol{R}$ are weighting matrices of the quadratic criteria designed experimentally with emphasis on the integral of the position error $e_{x_2}(k) = x_{ref}(k) - x_2(k)$. The incremental form of the control law is as follows:

$$\Delta u_c(k) = -\boldsymbol{K_{LQI}}\Delta\boldsymbol{x_i}^T(k), \tag{18}$$

where $\boldsymbol{K_{LQI}}$ is a feedback gain. The $\boldsymbol{K_{LQI}}$ design can be automated using the *lqi* function of the Control System Toolbox in MATLAB. The control input of the MLM is defined as:

$$u_c(k) = u_{c0} + \Delta u_c(k). \tag{19}$$

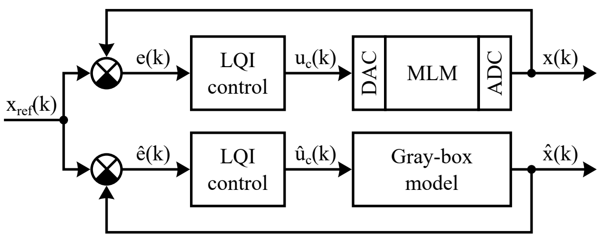

Fig. 9: Control structure of proposed LQI control for closed-loop validation of the Magnetic levitation model [27].

The closed-loop validation is based on comparing the behavior of real MLM $\boldsymbol{x}(k)$ with the gray-box model $\hat{\boldsymbol{x}}(k)$ in the control structure shown in Fig. 9. The designed control law (19) was first evaluated in the simulation environment. To simulate real conditions, an additive Gaussian noise was added and the ball speed $x_3(k)$ was estimated using the backward difference $x_3(k) = \Delta x_2(k)/T_s$, see Fig. 10. The simulation results are shown in Fig. 11. Clearly, the input voltage $u_c(k)$ is affected by the measurement noise, but the ball position $x(k)$ follows the reference trajectory $x_{ref}(k)$ well.

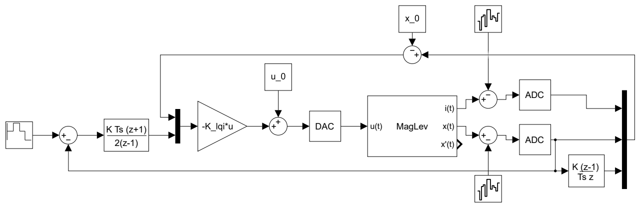

Fig. 10: Simulation structure for validation data generation.

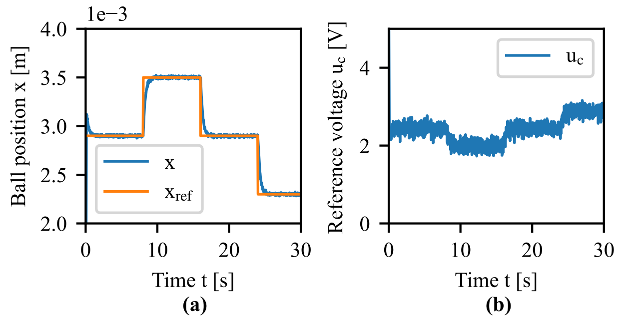

Fig. 11: Closed-loop validation using the LQI control law in the simulation environment; (a) system response; (b) system input.

A similar experiment was performed on the real MLM. The LQI control algorithm including the designed gain $\boldsymbol{K_{LQI}}$ was programmed into Board51 and the results are shown in Fig. 12. The input voltage $u_c(k)$ is still affected by the measurement noise but these results are comparable to the simulation. Although, the time it takes to reach the reference position $x_{ref}(k)$ is slightly longer compared to the simulation. It might be caused by unmodeled or simplified system dynamics, but further investigation is needed.

Validation results (Fig. 11 and Fig. 12) suggest the gray-box model is a suitable approximation of the real Modified MLM. Also, in conjunction with the proposed communication interface, it is considered to be a digital twin of the real system. The Aerodynamic [21] and Magnetic levitation models are both part of the R&D platform at CMCT&II and their digital twins open fur-

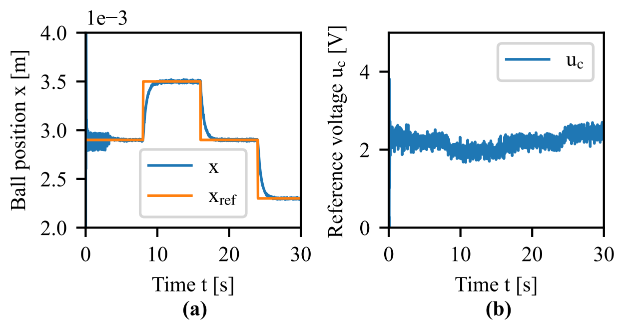

Fig. 12: Closed-loop validation using the LQI control law on the real system; (a) system response; (b) system input.

ther research possibilities in identification, control, and visualization tasks.

4. Conclusions

The paper's primary goal is to present system identification methodology in the structure of gray-box model on the Modified MLM. Firstly, a mathematical model of the MLM was derived using physics laws. Secondly, unknown parameter values of the model were estimated in the *MATLAB* environment using nonlinear experimental identification methods. Since the parameter estimation method could not handle systems with saturated outputs, data was split into multiple experiments. The resulting gray-box model structure was nonlinear and continuous in time. Lastly, the gray-box model was validated both in open-loop and closed-loop setups using the LQI control law. The LQI control law was designed based on a linear approximation of the gray-box model at the appropriate operation point. The validated gray-box model will be the basis for the digital twin of the MLM.

The modification of the MLM using the Board51 data acquisition board was presented. The Modified MLM was implemented into the first three levels of the DCS architecture. The presented implementation brings the controller closer to the system, which guarantees a constant sampling period. The Modified MLM is part of the research & development platform at CMCT&II and it will serve as a testbed for system identification and control algorithms design and evaluation.

In the future, improvements to step response time and state estimation could be further explored. Also, the gray-box model can be used to pre-train more complex black-box models such as neural networks for state estimation.

Acknowledgment

This work was supported by the Slovak Research and Development Agency under the contract No. APVV-19-0590.
This work has been supported by the project ALICE experiment at the CERN LHC: The study of strongly interacting matter under extreme conditions (ALICE KE TU 0410 / 2022).

Author Contributions

T.T. conceptualized the idea, designed the hardware interface, and implemented software modules. T.T. and A.J. developed the presented methodology. T.T. performed numerical calculations and simulations. J.J. supervised the MLM modification and secured funding using the ALICE TUKE project. A.J. and J.J. reviewed the article. All authors contributed to the article.

References

[1] YU, W. and X. LI. A Magnetic Levitation System for Advanced Control Education. *IFAC Proceedings Volumes*. 2014, vol. 47, iss. 3, pp. 9032–9037. ISSN 1474-6670. DOI: 10.3182/20140824-6-ZA-1003.00147.

[2] HAN, H.S. and D.S. KIM. *Magnetic Levitation: Maglev Technology and Applications*. Dordrecht: Springer Netherlands, 2016. ISBN 978-94-017-7524-3.

[3] DIVANDARI, M., M. HASHEMI-TILEHNOEE, M. KHALEGHI and M. HOSSEINKHAH. A Novel Control-rod Drive Mechanism via Electromagnetic Levitation in MNSR. *Nukleonika*. 2014, vol. 59, iss. 2, pp. 73–79. ISSN 1508-5791. DOI: 10.2478/nuka-2014-0008.

[4] MASUZAWA, T. Magnetically suspended motor system applied to artificial hearts and blood pumps. *Proceedings of the Institution of Mechanical Engineers, Part I: Journal of Systems and Control Engineering*. 2017, vol. 231, iss. 5, pp. 330–338. ISSN 0959-6518. DOI: 10.1177/0959651816640681.

[5] HUMUSOFT s.r.o. *CE 152 Magnetic Levitation Model*. Available at: `https://www.humusoft.cz/models/ce152/` (accessed 17 November 2022).

[6] SILVA, B.E. and R.S. BARBOSA. Experiments with Neural Networks in the Identification and Control of a Magnetic Levitation System Using a Low-Cost Platform. *Applied Sciences*. 2021, vol. 11, iss. 6, pp. 1–25. ISSN 2076-3417. DOI: 10.3390/app11062535.

[7] ŠUSTER, P. and A. JADLOVSKÁ. Application Results Identification Based on Genetic Algorithm in Nonlinear Control Design of Magnetic Levitation System. *Electroscope*. 2013, vol. 1, pp. 1–10. ISSN 1802-4564. Available at: `http://hdl.handle.net/11025/1883`.

[8] Magnetic Levitation: Quanser. Available at: https://www.quanser.com/products/magnetic-levitation/ (accessed 17 November 2022).

[9] Magnetic Levitation System: Feedback Instruments. Available at: https://www.feedback-instruments.com/pdf/brochures/33-026_Datasheet_MagneticLevitationSystem_LABVIEW_10_2013.pdf (accessed 17 November 2022).

[10] Magnetic Levitation System: Bytronic. Available at: https://www.bytronic.net/wp-content/uploads/2015/06/MLS-PL0111.pdf (accessed 17 November 2022).

[11] SLAVIK, D. and M. HYPIUSOVÁ. Toolbox for Modeling and Control of Magnetic Levitation System*. In: *2023 24th International Conference on Process Control (PC)*. Štrbské Pleso, Slovakia: IEEE, 2023, pp. 267–272. ISBN 979-8-3503-4763-0. DOI: 10.1109/PC58330.2023.10217769.

[12] JADLOVSKÝ, J., A. JADLOVSKÁ, S. JADLOVSKÁ, J. ČERKALA, M. KOPČÍK, J. ČABALA, M. ORAVEC, M. VARGA AND D. VOŠČEK. Research activities of the center of modern control techniques and industrial informatics. In: *14th International Symposium on Applied Machine Intelligence and Informatics*. Herľany: IEEE, 2016, pp. 279–285. ISBN 978-1-4673-8741-5. DOI: 10.1109/SAMI.2016.7423021.

[13] CHALUPA, P., M. MALÝ and J. NOVÁK. Nonlinear Simulink Model of Magnetic Levitation Laboratory Plant. In: *30th European Conference on Modelling and Simulation*. Regensburg: ECMS, 2016, pp. 293–299. ISBN 978-1-5108-2435-5. DOI: 10.7148/2016-0293.

[14] CHALUPA, P., J. NOVÁK and M. MALÝ. Modelling and model predictive control of magnetic levitation laboratory plant. In: *31st European Conference on Modelling and Simulation*. Budapest: ECSM, 2017, pp. 367–373. ISBN 978-0-9932440-4-9. DOI: 10.7148/2017-0367.

[15] DUŠEK, F., J. TUČEK, A. NOVOTNÝ and D. HONC. Generalized first-principle model of magnetic levitation. *Journal of Magnetism and Magnetic Materials*. 2023, vol. 587, iss. 171330, pp. 1–10. ISSN 0304-8853. DOI: 10.1016/j.jmmm.2023.171330.

[16] NOVOTNÝ, A. and D. HONC. Application of Model Predictive Controller to Magnetic Levitation. In: *2023 24th International Conference on Process Control (PC)*. Štrbské Pleso, Slovakia: IEEE, 2023, pp. 90–95. ISBN 979-8-3503-4763-0. DOI: 10.1109/PC58330.2023.10217631.

[17] HONC D. and E.R. SANSEVERINO. Magnetic Levitation–Modelling, Identification and Open Loop Verification. *Transactions on Electrical Engineering*. 2019, vol. 8, iss. 1, pp. 13–16. ISSN 1805-3386. DOI: 10.14311/TEE.2019.1.013.

[18] CHAMRAZ, Š., M. HUBA and K. ŽÁKOVÁ. Stabilization of the Magnetic Levitation System. *Applied Sciences*. 2021, vol. 11, iss. 21, pp. 1–14. ISSN 2076-3417. DOI: 10.3390/app112110369.

[19] KARUNASENA, G.M.K.B., H.D.N.S. PRIYANKARA and B.G.D.A. MADHUSANKA. Artificial Neural Network vs PID Controller for Magnetic Levitation System. *International Journal of Innovative Science and Research Technology*. 2020, vol. 5, iss. 7, pp. 505–511. ISSN 2456-2165. DOI: 10.38124/IJISRT20JUL432.

[20] HUMUSOFT s.r.o. *CE 150 Helicopter Model*. Available at: https://www.humusoft.cz/discontinued/ce150/ (accessed 30 October 2023).

[21] TKÁČIK, T., M. TKÁČIK, S. JADLOVSKÁ and A. JADLOVSKÁ. Design of Aerodynamic Ball Levitation Laboratory Plant. *Processes*. 2021, vol. 9, iss. 11, pp. 1–19. ISSN 2227-9717. DOI: 10.3390/pr9111950.

[22] JADLOVSKÝ, J., J. ČABALA, A. JADLOVSKÁ, S. JADLOVSKÁ, M. KOPČÍK, M. ORAVEC, M. TKÁČIK and D. VOŠČEK. A Novel General Purpose Data Acquisition Board with a DIM Interface. In: *16th Int. Conf. on Accelerator and Large Experimental Control Systems (ICALEPCS'17)*. Barcelona: JACoW, 2017, pp. 1565–1568. ISBN 978-3-95450-193-9. DOI: 10.18429/JACoW-ICALEPCS2017-THPHA076.

[23] PUGELOVÁ, Z. Review of Cyber-Physical Systems and their Architectures. In: *22rd Scientific Conference of Young Researchers*. Košice: Elfa, 2022, pp. 207–210. ISBN 978-80-553-4061-6. Available at: http://scyr.kpi.fei.tuke.sk/wp-content/scyr-files/history/SCYR_2022_Proceedings.pdf.

[24] LIU, M., S. FANG, H. DONG and C. XU. Review of digital twin about concepts, technologies, and industrial applications. *Journal of Manufacturing Systems*. 2021, vol. 58, iss. B, pp. 346–361. ISSN 1878-6642. DOI: 10.1016/j.jmsy.2020.06.017.

[25] LJUNG, L. *System Identification: Theory for the User*. Hoboken: Prentice Hall PTR, 1999. ISBN 978-0-13-656695-3.

[26] TKÁČIK, T. The Survey of Nonlinear Dynamical System Identification Methods. In: *22rd Scientific*

Conference of Young Researchers. Košice: Elfa, 2022, pp. 203–206. ISBN 978-80-553-4061-6. Available at: http://scyr.kpi.fei.tuke.sk/wp-content/scyr-files/history/SCYR_2022_Proceedings.pdf.

[27] TKÁČIK, T. *Software Modules for Modeling, Control and Simulation of Magnetic and Aerodynamic Levitation Educational Models*. Košice, 2021. Diploma Thesis. Technical univeristy of Košice. Supervisor: J. JADLOVSKÝ.

About Authors

Tomáš TKÁČIK (corresponding author) was born in 1998 and graduated (MSc) with honors in 2021 at the DCAI of the FEEI at TUKE. After graduation, he has become a PhD. student at the same department. His research is focused on classical and intelligent methods for nonlinear dynamic system identification of physics systems and model validation to design optimal identification methodology for systems at the CMCT&II and CERN.

Anna JADLOVSKÁ was born October 29th, 1960. She received her MSc. degree in the field of TC at the Faculty of Electrical Engineering of the TUKE in 1984. She defended her PhD thesis in the domain of Automatization and Control in 2001 at the same University; her thesis title was "Modelling and Control of Non-linear Processes Using Neural Networks". Since 1993 she worked at the DCAI FEEI TUKE as a Associate Assistant and since 2004 she has been working as an Associate Professor. Her main research activities include the problems of adaptive and optimal control – in particular predictive control with constraints for non-linear processes using neural networks and methods of artificial intelligence (Intelligent Control Design). She is the author of scientific articles and contributions to various journals and international conference proceedings, as well as being the co-author of some monographs.

Ján JADLOVSKÝ was born on June 13, 1960. He graduated in the field of Technical Cybernetics (TC) at Electrotechnical faculty of TUKE with focus on robotics. In the workplace of the speech recognition, he vindicated his dissertation work in 1990 and in 1994 he was habilitated for associate professor with his habilitation thesis dealing with DCS. Since 1994 he has worked at DCAI FEEI TUKE as assistant professor. His teaching activities are focused on the issues of proposal and implementation of distributed systems for control of the production processes. His research activities are oriented towards distributed control systems, image recognition, complex functional diagnostics of the controllers, diagnostics of production control systems, design of the information and control systems with application of the latest information technology. Currently he is Team Leader for TUKE for participation of TUKE in the ALICE Collaboration at CERN. He is a chief executive of company KYBERNETIKA, s.r.o., Košice.